Pergamon

Int. J. Heat Mass Transfer. Vol. 40, No. 17, pp. 4151–4159, 1997

Printed in Great Britain
0017-9310/97 $17.00+0.00

PII: S0017-9310(97)00030-6

Heat transfer in moving beds with a stagnant interstitial gas

OTTO MOLERUS

Lehrstuhl für Mechanische Verfahrenstechnik der Universität Erlangen-Nürnberg, Cauerstrasse 4, 91058 Erlangen, Germany

(*Received* 11 *June* 1996 *and in final form* 14 *January* 1997)

Abstract—The contact resistance for the heat transfer between adjacent particles is identified as the limiting factor for heat transfer in moving beds of particles consisting of rather hard solid materials and filled with a stagnant interstitial gas. It defines the short time heat transfer, which is determined by the thermal conductivity of the gas between the heated surface and the first row of particles, as well as the long time heat transfer which is characterized by the progression of the temperature front into the bulk of the bed. It also governs the steady heat conduction through a stationary bed kept at different temperatures at its ends. © 1997 Elsevier Science Ltd.

INTRODUCTION

In the literature, experimental results on the heat transfer between heated surfaces and moving beds are usually presented in the form of the mean heat transfer coefficient related to the heating surface area and as a function of the contact time of the particles. Heat transfer surfaces which are parallel to the direction of particle migration allow for a fairly accurate determination of the contact time. In industrial practice, however, submerged horizontal heat exchanger tubes are more typical and in this case the actual particle contact time may be more elusive, since the effective contact area now becomes a complex function of the flow around the tube. Using some typical numerical values an order of magnitude for contact times can be estimated. For instance the active contact circumference of a horizontally placed tube is about one diameter. Thus, for a tube diameter of 0.06 m and for particle migration velocities of 0.006–0.6 m s^{-1}, contact times of $0.1 \leqslant t \leqslant 10$ s are obtained.

A second configuration of practical interest is the heat transfer between submerged surfaces and bubbling fluidized beds. Recently, direct measurements of contact times between submerged surfaces and particles in bubbling fluidized beds have been reported [1]. These experimental results indicate that the particles slide along the heat transfer surface in the form of packets consisting of a multiplicity of particles, which occasionally are swept away by rising gas bubbles. At conditions yielding a maximum heat transfer to the bubbling fluidized bed particle contact times in the range of $0.3 \leqslant t \leqslant 1.5$ s have been observed [1]. Thus, moving bed heat transfer within this range of contact times can be regarded as a so to speak rudimentary version of bubbling fluidized bed heat transfer. Thus, from the point of view of engineering applications, a range of moving bed contact times of about $0.1 \leqslant t \leqslant 10$ s appears to encompass most cases of practical interest.

Heat transfer in moving beds has been discussed by several authors (see e.g. [2–6]). In these papers, the heat transfer coefficients are correlated by a contact resistance model, whereby the bed of particles is considered as a continuum and the heat transfer between the bed and a heating surface is controlled by a contact resistance.

In the present paper it will be shown through evaluation of measurement data published in the literature, that in fact a contact resistance for the heat transfer between adjacent particles and/or between the heated surface and the particles is more precisely the decisive factor for the heat transfer between a heating surface and a moving bed consisting of rather hard particles and filled with a stagnant interstitial gas. Building on this foundation the main heat transfer properties of the bed can be described, namely:

(1) the contact resistance between the heating surface and the particle bed at rather short contact times;

(2) the heating up of moving beds during the progression of the temperature front into the bulk of the bed;

(3) the steady-state heat conduction through a stationary bed kept at different temperatures at its two ends.

SIMPLIFYING ASSUMPTIONS

The aim of this paper is not to achieve the utmost accuracy, but to reveal the essential features not easily identifiable with more lengthy calculation procedures. Thus, the following simplifying assumptions are *a priori* introduced and their approximate validity is

NOMENCLATURE

C	constant	$\tilde{R}$	gas constant [Nm mol^{-1} K^{-1}]
c_p	specific heat of particle material [Ws kg^{-1} K^{-1}]	s	size of surface asperities [m]
d_p	particle diameter [m]	s_{min}	minimum effective surface roughness [m]
h	heat transfer coefficient [W m^{-2} K^{-1}]	t	time [s]
k_e	effective thermal conductivity [W m^{-1} K^{-1}]	T	absolute temperature [K]
k_g	gas thermal conductivity [W m^{-1} K^{-1}]	γ	accommodation coefficient
k_p	solid material thermal conductivity [W m^{-1} K^{-1}]	μ	viscosity [kg m^{-1} s^{-1}]
ℓ	distance [m]	ρ_p	particle density [kg m^{-3}]
ℓ_0	mean free path of gas molecules [m]	φ	angle.
$\tilde{M}$	molar mass [kg mol^{-1}]		
p	pressure [Nm^{-2}]		
r	integration variable [m]		
R	radius [m]		

Dimensionless groups

$Co = k_g C s_{min} t/\rho_p c_p d_p^3$ [dimensionless contact time]

$Nu = h d_p/k_g$ [Nusselt number].

checked retroactively by comparison with experiments:

(1) Insignificance of the volumetric heat capacity of the interstitial gas is assumed. This assumption is rather trivial for a stagnant interstitial gas, because as a rule, the volumetric heat capacity of the interstitial gas is rather low in comparison with that of the solid material, and the volumes of gas and solid are nearly equal in a particle bed with, e.g. a void fraction of about 0.4.

(2) The void fraction is not introduced as a model parameter, because for particle sizes $d_p \geqslant 100\ \mu$m it rarely varies much from $\varepsilon \approx 0.4$. Furthermore, the actual local void fraction at the heating surfaces is not available from the data given in the literature published on the subject.

(3) Insignificance of the solid material thermal conductivity in comparison with that of the interstitial gas. This assumption attributes any form of conductive resistance to the interstitial gas and is justified since the thermal conductivity of the interstitial gas is much lower than that of the solid material. There exists a simple experimental check for the proof of this assumption. If the heat conduction in a particle bed is only marginally improved by a drastic increase in the thermal conductivity of the solid material, e.g. by exchanging ceramic spheres by steel spheres, then the assumption is obviously valid.

From the point of view of modeling the heat transfer in particle beds, the last assumption is extremely stringent. It inherently postulates nothing less than temperature constancy in the entire volume of any individual particle. Thus, in the strict sense, any mode of heat transfer in a particle bed must then be close to the idealized model, whereby two adjacent particles in the main direction of heat flux are at two distinctly different temperature levels, and the heat transfer between them is due to a near jump-like temperature gradient in the gap between them. Furthermore, heat transfer through solid material paths between adjacent particles is inherently ignored. This last assumption holds true only for rather hard solid materials.

THE CONTACT RESISTANCE

In the literature two different physical reasons are given for the contact resistance observed with particle beds. For perfect spherical particles in contact with a plane wall, Schlünder [5] attributes the contact resistance to a diminished heat transfer rate in the gas in the region where the distance between the particle and the surface is less than the mean free path of the interstitial gas. Glosky *et al.* [6] attribute it to the surface roughness. Both approaches, however, are not contradictory, but instead complementary. Applying the same simplifying assumptions to the surface roughness model as Schlünder did for his mean free path model consists (see Fig. 1) in taking the distance $\ell = (d_p/2)(1-\cos\varphi)+s$ as decisive for the local heat transfer. Furthermore, it is assumed that a particle touching the heated surface is responsible for the energy transfer from the adjacent heated surface over an effective area of d_p^2. That part of the energy which is transferred within the surface area with the radius $0 \leqslant R \leqslant d_p/2$, in terms of a Nusselt number, is then

$$Nu(2R/d_p) \equiv \frac{h d_p}{k_g} = \pi \int_0^{2R/d_p} \frac{\left(\frac{2r}{d_p}\right) d\left(\frac{2r}{d_p}\right)}{1+\frac{2s}{d_p}-\sqrt{1-\left(\frac{2r}{d_p}\right)^2}}. \quad (1)$$

Integration of equation (1) yields

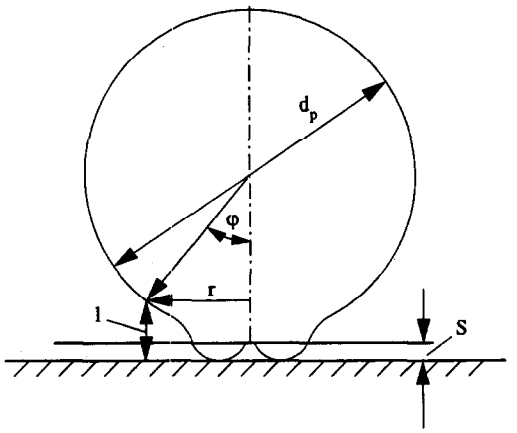

Fig. 1. Surface asperities model for short contact time heat transfer.

$$Nu[(2R/d_p)^2] = \pi\left\{\left(1+\frac{2s}{d_p}\right)\ln\left[1+\frac{d_p}{2s}(1-\sqrt{1-(2R/d_p)^2})\right] - [1-\sqrt{1-(2R/d_p)^2}]\right\}. \quad (2)$$

The heat transfer per particle then is defined by $2R/d_p \to 1$, i.e. by the maximum Nusselt number for short contact time

$$Nu_{max} \equiv \frac{h_{max}d_p}{k_g} = \pi\left[\left(1+\frac{2s}{d_p}\right)\times\ln\left(1+\frac{d_p}{2s}\right)-1\right]. \quad (3)$$

According to Schlünder's approach, for ideal geometries

$$s_{min} = 2\ell_0\frac{2-\gamma}{\gamma} \quad (4)$$

where ℓ_0 designates the mean free path of the gas molecules and γ the accommodation coefficient. The accommodation coefficient γ defines that fraction of the gas molecules which are not reflected, when hitting a solid surface. Equation (4) reveals that the physics of gases yields a minimum effective roughness s_{min}, below which particles can be considered thermodynamically smooth. Thus, Schlünder's approach provides an upper bound for the maximum Nusselt number.

MATERIAL PROPERTIES OF MODEL SYSTEMS USED WITH EXPERIMENTAL INVESTIGATIONS

The mean free path of the gas molecules is (see e.g. [5])

$$\ell_0 = \frac{16}{5}\sqrt{\frac{\tilde{R}T}{2\pi\tilde{M}}}\frac{\mu}{p} \quad (5)$$

with the gas constant $\tilde{R}$, the absolute temperature T, the molar mass $\tilde{M}$, the viscosity μ, and the pressure p.

In Table 1 the properties of three different gases are tabulated, which have been used in key experiments, to be discussed below. Table 1 reflects the significance of their differing properties. The change from the refrigerant CCl_2F_2 to air ($\approx$ nitrogen) increases the thermal conductivity by a factor of about 2. The increase in the mean free path length at unchanged accommodation coefficient of 0.9 increases the minimum effective roughness s_{min} by a factor of about 2.6. Replacing air by helium results in a very significant increase in the effective minimum roughness s_{min}, mainly due to the drastically reduced accommodation coefficient of helium. The gas thermal conductivity is increased by a factor of 6.5. Table 2 summarizes the thermal conductivity and the heat capacity of the solid materials used in the experiments. In particular the thermal conductivity exhibits a vast variation between experiments.

THE EFFECTIVE THERMAL CONDUCTIVITY OF PARTICLE BEDS

The model formulation given above can now be used without modification to also describe the effective thermal conductivity of particle beds (compare Fig. 1). For two adjacent spheres in a cubic array in the main direction of heat flux, the relevant distance for the heat conduction is the particle diameter, the distances ℓ in the model must simply be doubled to yield the gap between particles. The relevant cross-section for the heat flux is the particle equatorial area $(\pi d_p^2)/4$. Thus, the ratio of effective to gas thermal conductivity is given by the equation

$$k_e/k_g = (2/\pi)Nu_{max} = 2\left[\left(1+\frac{2s}{d_p}\right)\ln\left(1+\frac{d_p}{2s}\right)-1\right]. \quad (6)$$

Both equations (3) and (6) indicate that the heat transfer in a particle bed is a function of only the length ratio s/d_p. The inherent concept is that the sole physical reason for short contact time resistance between a heating surface and a particle bed as well as for steady-state heat conduction inside the bed is practically exclusively the contact resistance in the gap between the contacting solid bodies. In other words $h_{max} \to 0$ as well as $k_e \to 0$ for $k_g \to 0$. As a practical consequence it follows that the short contact time resistance can be immediately deduced, within reasonable limits of accuracy, from measurements of the steady-state heat conduction in the particle bed. Both equations (3) and (6) assume insignificance of the heat conduction through solid paths between adjacent particles. The solid materials listed in Table 2 are all more or less rather hard. In that case, due to the small contact surface, the heat conduction through direct solid paths is expected to be insignificant. This sup-

Table 1. Properties [7] of the gases used in key experiments

Gas	T [K]	p [bar]	k_g [W (mK)$^{-1}$]	ℓ_0 [μm]	γ	s_{min} [μm]
CCl_2F	325	1	0.0111	0.027	0.9	0.066
Air (nitrogen)	293	1	0.026	0.07	0.9	0.17
Helium	325	1	0.17	0.21	0.3	2.5

Table 2. Properties [7] of the solid materials used in key experiments

Solid material	k_p [W(mK)$^{-1}$]	$\rho_p c_p$ [(Ws) (m^{3}K)$^{-1}$]
Ceramic	1.2	1.67×10^6
Glass	0.8	2×10^6
Sand	0.58	2×10^6
Uranium	26	—
Steel	40	3.6×10^6
Copper	385	3.47×10^6

position is fully confirmed by extensive experimental data reported in [7]. In nearly all cases the particle bed thermal conductivity at vacuum conditions ($p \leqslant 1$ N m^{-2}) was less than one tenth of the value which was measured at ambient pressure ($p = 10^5$ N m^{-2}).

In Table 3, predictions according to equation (3) or (6) are compiled for ideal spheres in air (nitrogen) at ambient conditions. The predictions according to Table 3 fit quite reasonably to experimental data reported in [7] with $k_e/k_g \approx 9$ for 50 μm ceramic spheres in nitrogen, $k_e/k_g \approx 11$ for 190 μm uranium spheres in nitrogen and $k_e/k_g \approx 20$ for 3.18 mm steel spheres in air (all at ambient conditions with respect to pressure and temperature). The corresponding broad range of solid material thermal conductivities ($k_p \approx 1.2$ W (m K)$^{-1}$ for ceramics, $k_p = 40$ W (m K)$^{-1}$ for steel) at the same time confirms the postulated insignificance of solid material conductivity.

The strong significance of the length ratio s_{min}/d_p for the heat transfer in particle beds becomes obvious from results which have been obtained from experiments with an unchanged particle bed in the presence of different interstitial gases. A comparison of the predictions according to equation (6) with experimental data [7] for steel spheres ($d_p = 1.8$ mm) in CCl_2F_2, nitrogen and helium is given in Table 4. From the comparisons given in Tables 3 and 4 it can be concluded that equation (6), which is presented in Fig. 2, provides a reasonable approximative equation for the thermal conductivity of particle beds in the presence of an interstitial gas.

Table 4. Effective thermal conductivity, comparison between measurement [7] and prediction according to equation (6) for steel spheres ($d_p = 1.8$ mm) in different gases at ambient conditions with respect to pressure and temperature

Gas	(k_e/k_g) measured	(k_e/k_g) (equation 6)
CCl_2F_2	18	17
Nitrogen	16	15.1
Helium	10	9.8

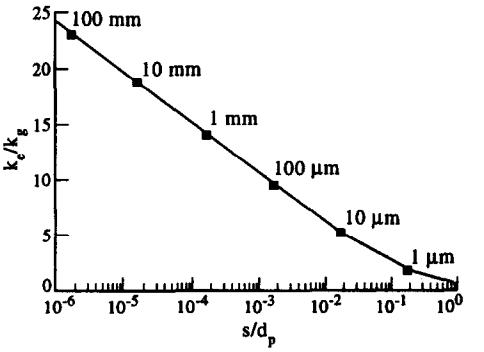

Fig. 2. Effective thermal conductivity in particle beds according to equation (6). Numerical values of diameter represent ideal spheres in air (nitrogen) at ambient conditions.

LIMITING CASES OF HEAT CONDUCTION IN PARTICLE BEDS

The results presented up to now indicate that both ends of the spectrum of particle bed heat transfer, namely short contact time maximum heat transfer as well as steady-state heat conduction after heating up, are physically related to the same mechanism, namely contact resistance for the heat transfer between adjacent particles or between a particle and a plane surface.

The role of contact resistance is best understood from inspection of equations (2) and (3). Division of equation (2) by equation (3) yields the relative contribution of the area with the radius R around the particle's contact point to the total heat transfer per particle

Table 3. Particle diameter d_p, length ratio s_{min}/d_p, Nusselt number Nu_{max} and dimensionless effective thermal conductivities k_e/k_g for particle beds in air (nitrogen) at ambient conditions

d_p [μm]	10	10^2	10^3	10^4
s_{min}/d_p	1.7×10^{-2}	1.7×10^{-3}	1.7×10^{-4}	1.7×10^{-5}
Nu_{max} equation (3)	7.65	14.35	22	29.2
k_e/k_g equation (6)	4.85	9.15	14	18.6

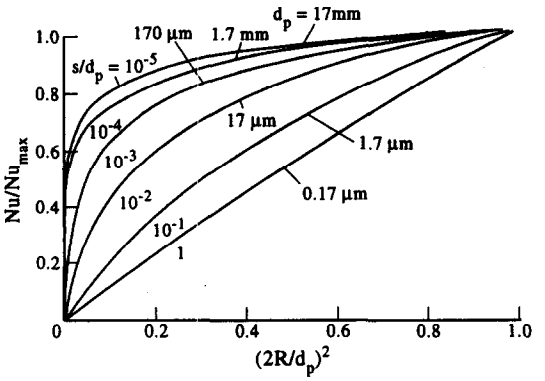

Fig. 3. Relative contribution of the area with radius R to the total heat transfer per particle. Particles are smooth spheres in air at standard conditions.

$$\frac{Nu[(2R/d_p)^2]}{Nu_{max}} = \frac{(1+2s/d)\ln\{1+(d_p/2s)[1-\sqrt{1-(2R/d_p)^2}]\}}{(1+2s/d)\ln[1+(d_p/2s)]-1} - \frac{[1-\sqrt{1-(2R/d_p)^2}]}{(1+2s/d_p)\ln[1+(d_p/2s)]-1}. \quad (7)$$

In Fig. 3, equation (7) is plotted in the form of $Nu[(2R/d_p)^2]/Nu_{max}$ with s/d_p as parameter. The computations have been performed for the thermodynamically smooth spheres in air at standard conditions. Figure 3 reveals that for $s/d_p \leqslant 10^{-3}$ the relative area $(2R/d_p)^2 \leqslant 0.3$ contributes more than 80% of the total heat transfer. On the other hand, for $s/d_p \geqslant 10^{-2}$ the local heat transfer approaches independence of the radial position, which is almost achieved for $s/d_p = 1$.

This peculiar property of heat transfer between a heated surface and adjacent particles, or between contacting particles is the result of the mutual interaction of two different physical causes, namely:

(1) Decrease of the heat transfer in those areas where the mean free path of the gas molecules exceeds the gap width. According to equation (4), this effect is intensified by a low accommodation coefficient.

(2) Degradation of the heat transfer with increasing gap width.

From the mutual interaction of these two different tendencies the existence of two limiting cases can be postulated, as depicted schematically in Fig. 4.

For $s/d_p = 1$ the heat transfer in the entire space between adjacent particles is solely defined by the effective mean free path length s_{min} of the gas molecules according to equation (4) because with $s \approx d_p$ surface asperities are no longer relevant. In that case the heat transfer is evenly distributed over the gap between adjacent particles. Evaluation of measurements indicate that this limiting case is attained for $s/d_p \geqslant 1.7 \times 10^{-2}$.

For $s/d_p \to 0$ heat conduction is confined to the region in close proximity to the contact point, because outside this region the larger gap results in an effective thermal insulation. The evaluation of measurements will show, that this limiting case is attained for $s/d_p \leqslant 1.7 \times 10^{-3}$. Between these two limiting cases, a gradual transition in the intermediate regime $1.7 \times 10^{-3} \leqslant s/d_p \leqslant 1.7 \times 10^{-2}$ can be expected.

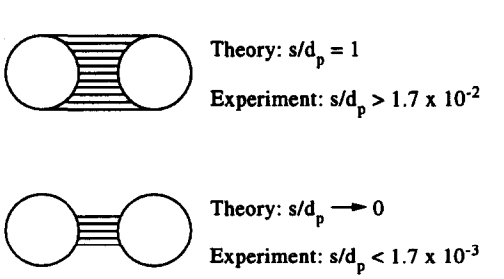

Fig. 4. The two limiting cases of heat conduction between adjacent particles.

MOVING BED HEAT TRANSFER, DIMENSIONAL ANALYSIS

The most peculiar manifestation of the role of the length ratio s/d_p is observed with the heat transfer between a heated solid surface and a particle bed sliding alongside of it. With a short contact time, a maximum Nusselt number according to equation (3) is observed, whereas with progression of the temperature front inside the bulk of the bed, a long contact time variant of the heat transfer is attained, which is characterized by gradual heating up of the bed.

As already shown in the preceding section both ends of the spectrum of particle bed heat transfer modes, namely short contact time heat transfer and steady-state heat conduction, depend on the length ratio s/d_p. Therefore, inevitably the intermediate situation, namely gradual heating up of a moving bed must depend also on the length ratio s/d_p. On the other hand, as already shown, short contact time heat transfer in the form of $Nu_{max} = Nu_{max}(s/d_p)$ as well as steady heat conduction in the form of $k_e/k_g = k_e/k_g(s/d_p)$ according to equation (6), describe basically the same heat transfer mechanism, i.e. both are defined by an interrelation between two dimensionless groups. For moving bed heat transfer with progression of the temperature front into the bulk of the particle bed an additional property of the materials involved becomes significant, namely the solid material storage capacity for thermal energy in the form of the volumetric specific heat $\rho_p c_p$. From this fact it follows, conclusively, that in general, moving bed heat transfer must be defined by an interrelation among three dimensionless groups. It will be shown that an interrelation between only two dimensionless groups, as usually assumed (see e.g. [5]), holds true only for the two limiting cases of $s/d_p \to 1$, and $s/d_p \to 0$.

Heat transfer from a heating surface of a moving

bed depends, therefore, on the following influencing factors.

Particle data

(1) Particle size d_p [m]

(2) Volumetric heat capacity of the solid material $\rho_p c_p$ [(W K^{-1}) m^{-1}].

Gas data

(3) Thermal conductivity of the interstitial gas k_g [(W K^{-1}) m^{-1}].

Data of the heat transfer in the gap between adjacent particles

Either a particle property

(4a) surface asperities s [m] in the case of $s > s_{min}$; or

(4b) effective surface roughness s_{min} [m] in the case of thermodynamically smooth particle surfaces ($s < s_{min}$).

The effective surface roughness according to equation (4) is a clear function of only the gas properties, i.e. the influencing factor s is an ambiguous property.

Experimental parameters

For a given length of the heat transfer surface

(5) contact time t [5].

Desired quantity

(6) Mean heat transfer coefficient h [(W K^{-1}) m^{-2}] related to the heating surface area.

Further to these governing parameters, and as a consequence of the above discussion with respect to short contact time heat transfer and steady-state heat conduction, it is assumed that for the progression of the temperature front into the bulk of the bed:

(1) there exists no significant contribution to the energy transfer by heat conduction along solid paths between adjacent particles, so that the solid material thermal conductivity k_p remains irrelevant;

(2) heat storage capacity of the gas is also irrelevant, since $\rho_g c_g \ll \rho_p c_p$; and

(3) particle bed void fraction is not introduced as an additional parameter ($\varepsilon \approx 0.4$ for $d_p \geqslant 100$ μm).

According to the Buckingham π theorem with three basic dimensions (W K^{-1}; m; s; compare the influencing factors 1–6) and with six influencing factors, just three dimensionless groups can be derived. A possible choice is the Nusselt number $Nu \equiv (hd_p)/k_g$, the length ratio s/d_p and a dimensionless contact time in the form of $(k_g t)/(\rho_p c_p d_p^2)$.

In the context of heat transfer problems, the choice of the Nusselt number certainly does not need any justification. The significance of the length ratio s/d_p is apparent by the already described short contact time heat transfer and steady-state heat conduction. The dimensionless contact time deserves, however, closer inspection.

MOVING BED HEAT TRANSFER, THE LIMIT $s/d_p \to 1$

Rearrangement of the dimensionless contact time yields

$$\frac{k_g t}{\rho_p c_p d_p^2} \equiv \frac{(k_g/d_p)d_p^2}{(\rho_p c_p d_p^3)/t}. \tag{8}$$

In the form given on the right-hand side of equation (8) the denominator describes exactly the storage capacity of a particle for thermal energy per unit of temperature difference and time t. The nominator on the other hand, is equivalent to the heat flux per area d_p^2 over a nominal gap of length d_p. This interpretation of the dimensionless contact time can be associated with case a of Fig. 4, in which an evenly distributed heat transfer over the gap between contacting particles is postulated, i.e. to the limit $s/d_p \to 1$. In this case the ratio s/d_p, by definition, is no longer a separate dimensionless variable. Therefore, in the limit $s/d_p \to 1$, there remain only two dimensionless variables, namely the Nusselt number and the dimensionless contact time, equation (8).

With progression of the temperature front into the bulk of the particle bed, a continuum-like behaviour, i.e. insignificance of particle size has been postulated [5]. The particle size can be eliminated through the following:

$$Nu^2 \frac{k_g t}{\rho_p c_p d_p^2} \equiv \frac{h^2 t}{k_g \rho_p c_p} = \text{const.} \tag{9}$$

According to Fig. 2, $k_e \approx k_g$ for $s/d_p \approx 1$, thus

$$\frac{h^2 t}{k_e \rho_p c_p} = \text{const.} \tag{10}$$

Furthermore, with $s/d_p \to 1$ certainly not the surface asperities, but instead s_{min} according to equation (4), i.e. the gas properties, define the thermal conduction in the gap between adjacent particles. Inspection of Table 1 reveals the largest values $s_{min} = 2.5$ μm for helium as interstitial gas.

In Fig. 5 experimental results reported by Harakas and Beatty [8] for glass beads and Al_2O_3 powder in

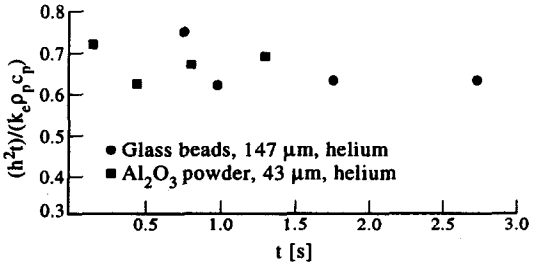

Fig. 5. Wall-to-bed heat transfer coefficients for moving beds in helium according to Harakas and Beatty [8].

helium are depicted in the form of equation (10) as a function of the contact time $0.2 \leqslant t \leqslant 2.7$ s. For such fine grained particles, contact times $t \geqslant 0.2$ s exceed that range of contact times, where a maximum Nusselt number according to equation (3) is observed. Therefore, Fig. 5 confirms equation (10) within plausible limits of experimental accuracy. From Fig. 5, it can be concluded that the theoretical limit $s/d_p \to 1$ is in practice already attained for $s_{min}/d_p \geqslant 2.5/147 = 1.7 \times 10^{-2}$.

MOVING BED HEAT TRANSFER, THE LIMIT $s/d_p \to 0$

The previous results, together with the computations shown in Fig. 3 suggest that there also exists a particular solution for case b of Fig. 4, i.e. for $s/d_p \to 0$. This expectation is confirmed by experimental results obtained with glass beads ($d_p = 150$, 400 and 600 μm) in air, as reported by Ernst [9] and as shown in Fig. 6. Figure 6 reveals the following facts:

(1) For contact times $t \leqslant 0.2$ s the transition towards the short contact time solution with Nu_{max} according to equation (3) is observed, namely decreasing heat transfer coefficient with increasing particle diameter.

(2) For contact time $t \geqslant 0.5$ s, the heat transfer is defined by the progression of the temperature front into the bulk of the bed. This feature is obvious from the independence of the heat transfer coefficient of particle size. In sharp contrast to equation (9) and Fig. 5, Fig. 6 reveals a time dependence $\sim t^{-1/3}$.

This observation demands a reconsideration of the dimensionless contact time, defined by equation (8). According to Fig. 4, case b, it is assumed that in the limit $s/d_p \to 0$ the thermal conductivity in the gap between adjacent particles is defined by the ratio k_g/s and the cross-sectional area relevant for the heat conduction is $\sim s^2$. Thus, the nominator of the dimensionless contact time is now $(k_g/s)s^2$. The storage capacity for thermal energy, however, remains unchanged, i.e. the denominator remains as $(\rho_p c_p d_p^3)/t$. Thus, in the limit $s/d_p \to 0$, instead of equation (8), an appropriate definition of a dimensionless contact time is:

$$\frac{(k_g/s)s^2}{(\rho_p c_p d_p^3/t)} \equiv \frac{k_g s t}{\rho_p c_p d_p^3}. \tag{11}$$

Insignificance of the particle diameter for longer contact times, as indicated by the experimental results depicted in Fig. 6, then requires

$$Nu \sqrt[3]{\frac{k_g s t}{\rho_p c_p d_p^3}} \equiv h \sqrt[3]{\frac{s t}{k_g^2 \rho_p c_p}} = \text{const.} \tag{12}$$

Also in agreement with the experimental results shown in Fig. 6, equation (12) predicts dependency $h \sim t^{-1/3}$.

With $s/d_p \to 0$ and with e.g. air at ambient conditions as interstitial gas ($s_{min} = 0.17$ μm), an additional complication can be envisioned. A characteristic length of the order ≈ 0.1 μm is also commensurate with the size of surface asperities of spherical particles. With non-spherical particles, therefore, the effective surface asperities exceed s_{min}, i.e. $s > s_{min}$. With evaluation of experimental data, therefore, it is questionable whether the gas property, s_{min} or particle properties s are more relevant. The aim of this paper, however, is to elucidate basic features, not normally revealed by fitting parameters in the form of unproven or arbitrary assumptions. Conforming to this aim, the following formal procedure is followed. The right-hand side of equation (12) is split into two constants k, C in the form

$$Nu \sqrt[3]{\frac{k_g s t}{\rho_p c_p d_p^3}} = \frac{K}{C^{1/3}}. \tag{13}$$

Rearrangement of equation (13) and assuming $s = s_{min}$ yields

$$Nu \sqrt[3]{\frac{k_g C \times s_{min} t}{\rho_p c_p d_p^3}} = K. \tag{14}$$

Equation (14) now is interpreted in the following way. In a strict sense, dominance of the gas properties leads to $C = 1$, whereas significance of surface asperities leads to $C > 1$. In a pragmatic approach this sophistication is ignored. Instead, one set of measurement data is used in order to define a dimensionless contact time

$$Co = \frac{k_g C \times s_{min} t}{\rho_p c_p d_p^3} \tag{15}$$

by putting $K = 1$. This procedure yields a numerical value $C \times s_{min}$ [μm]. Experimental results are represented by plotting Nu as a function of $Co^{1/3}$. Results obtained from other investigations then may result in constants $K \neq 1$. On a log/log scale, this would correspond to straight lines with identical slopes -1, but with a parallel shift. This shift can be attributed to the following two physical reasons:

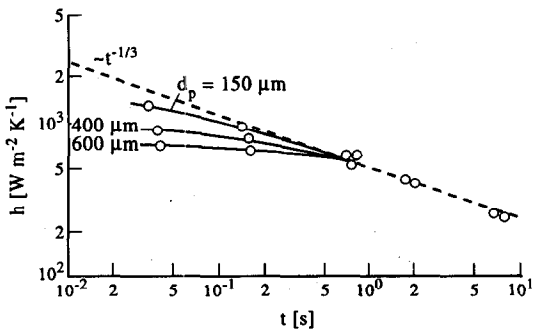

Fig. 6. Wall-to-bed heat transfer coefficients according to Ernst [9].

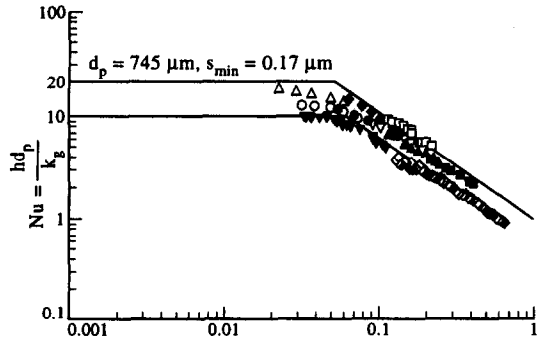

Fig. 7. Nusselt number as a function of the cube root of the dimensionless contact time; $C \times s_{min} = 6.5$ μm. Measurements taken from [8, 10, 11].

(1) differences in the, generally unknown, numerical values of s;

(2) differences in the particle bed void fractions.

Figure 7 shows earlier measurements reported by Botterill *et al.* [10] as well as more recent experimental results presented by Barreto *et al.* [11]. In these experiments the interstitial gas was air at standard pressure and temperature. All particle sizes exceeded 100 μm, therefore, $s_{min}/d_p < 1.7 \cdot 10^{-3}$. The experimental results indicate that $Nu \propto Co^{-1/3}$, thus the long contact time solution appears to be applicable, where the heat transfer is concentrated in the immediate vicinity of the contact points (see Fig. 3).

The numerical value $C \times s_{min} = 6.5$ μm has been found from the experimental data of Ref. [10]. Both investigations, Ref. [10] as well as Ref. [11] verify $Nu \propto Co^{-1/3}$ for the long contact time asymptotic solution, nevertheless some distinguishing factors can be identified. The measurement data of Ref. [10] comprise real contact times mostly in the range of $0.2 \leqslant t \leqslant 1$ s, so that the variation in the dimensionless contact time, Co, was mainly achieved by variation of the particle size, $110 \leqslant d_p \leqslant 745$ μm and the volumetric heat capacity $\rho_p c_p$ of the solid material.

The broadest variation of the dimensionless contact time Co is exhibited by the measurement data of Ref. [11]. The longest real contact time of the experiments with the 500 μm glass particles was $t \approx 6$ s and, hence, the cube root of the longest dimensionless contact time $\propto t^{1/3}/d_p \approx 3.7$ s$^{1/3}$ mm^{-1}. The shortest real contact time for the 115 μm silicate particles was $t \approx 0.05$ s, and, hence the cube root of the shortest dimensionless contact time $\propto 3.2$ s$^{1/3}$ mm^{-1}. Thus, since the volumetric heat capacity of both solid materials is the same, the measurement data for both particle sizes show only a short overlapping region when plotted as a function of the cube root of the dimensionless contact time.

From Fig. 7, the following features are indisputable:

(1) The measurement data obtained from the 500 μm glass particles extend down exactly into the short contact time regime with $Nu_{max} = 10$. The measurement data of the 115 μm silicate particles extend far into the long contact time regime. Both measurement series lead to a single straight line with a slope of -1 in Fig. 7. This line, shown as a dashed line in Fig. 7, extends over one decade of the cube root of Co, i.e. over no less than three decades of Co itself.

(2) For a particle size of $d_p = 745$ μm and for air at standard conditions, i.e. for $s_{min} = 0.17$ μm, a maximum Nusselt number of $Nu = 20$ is predicted. The measurement data of Ref. [10] just attain Schlünder's upper bound Nu_{max}.

(3) The significance of the gas thermal conductivity in equation (14) is confirmed by experimental results reported by Harakas and Beatty [8] (380 μm glass beads in CCl_2F_2, temperature 350 K, $k_g = 0.0111$ W m^{-1} K^{-1}, mean free path of the gas molecules $\ell_0 = 0.027$ μm, accommodation coefficient $\gamma = 0.9$, thus, according to equation (4) $s_{min}/d_p = 1.74 \times 10^{-4}$).

MOVING BED HEAT TRANSFER, THE REGIME $1.7 \times 10^{-3} \leqslant s_{min}/d_p \leqslant 1.7 \times 10^{-2}$

As shown in the preceding paragraphs, evaluation of experiments yield, that the limit $s/d_p \to 1$, i.e. heat transfer evenly distributed over the gap between adjacent particles is attained in practice for values $s_{min}/d_p \geqslant 1.7 \times 10^{-2}$, whereas the limit $s/d_p \to 0$, i.e. concentration of the heat transfer around the contact point is attained in practice for $s_{min}d_p \leqslant 1.7 \times 10^{-3}$. In these two limiting cases the length ratio s/d_p is present in the form of two distinctly different time scalings of the heat transfer ($h \sim t^{-1/2}$ in the case $s/d_p \to 1$, $h \sim t^{-1/3}$ in the case of $s/d_p \to 0$). For the intermediate regime $1.7 \times 10^{-3} \leqslant s_{min}/d_p \leqslant 1.7 \times 10^{-2}$, a gradual shift in the exponent n of the function $h \sim t^{-n}$ must be expected such that $1/3 \leqslant n \leqslant 1/2$, i.e. increasing n with increasing s_{min}/d_p. This expectation is confirmed by the experimental results reported by Harakas and Beatty [8] (see Fig. 8). The contact times of their experiments fall within the range $0.15 \leqslant t \leqslant 3$ s. Only one of their experimental runs attained the short contact time limit, i.e. the Nu_{max} regime. So that the remaining experimental runs show no change in the slope of the log/log representations. Excluding the one experimental run, all other experimental observations gave a numerical value of $n = \text{const} > 0$ for gases at standard pressure. This means that all measurements belong to that regime, where the short contact time

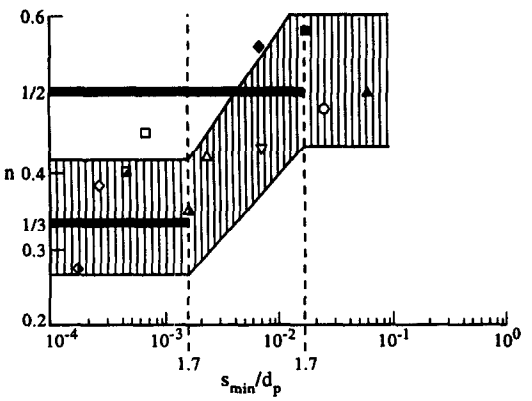

dp [μm]	In helium	In air	In CCl_2F_2
4	—	○	—
14	—	▽	—
43	▲	△	▲
147	■	□	◪
380	◆	◇	◆

Fig. 8. Measured exponents n, experimental data from [8].

solution ($n = 0$) is definitely left. By admitting an experimental inaccuracy of ± 0.1 in the determination of the exponent n, the data presented in Fig. 8 confirm a transition from $n \approx 1/3$ to $n \approx 1/2$ within the regime $1.7 \times 10^{-3} \leqslant s_{min}/d_p \leqslant 1.7 \leqslant 10^{-2}$.

CONCLUSIONS

(1) With respect to moving beds. Particle packings in the presence of a stagnant interstitial gas can be treated as a sequence of convex bodies in mutual near-point contacts for rather hard solid materials. This model is capable of qualitatively accounting for the short time heat transfer as well as the steady-state heat conduction in particle beds. The heat transfer from heating surfaces to moving beds is identified to provide the most significant manifestation of contact resistance.

(2) With respect to bubbling fluidized beds. Direct correspondence between moving bed heat transfer and heat transfer in bubbling fluidized beds is not likely to be expected, i.e. the equations derived in this paper cannot be extended to the prediction of heat transfer in bubbling fluidized beds, because there exist also significant differences, for instance no firm mutual particle contacts in the case of fluidized beds. However, in a less strict sense, it seems legitimate to deduce certain expectations from the derived results. These are:

(a) With respect to the heat transfer in fluidized beds consisting of fine-grained particles (particle size generally $d_p \leqslant 100$ μm at standard conditions). The heat transfer dominated by the transient heating (or cooling) of larger particle aggregates, consisting of a multiplicity of primary particles. Therefore, both the heat capacity of the particulate material and the gas thermal conductivity are expected to be significant parameters.

(b) With respect to the heat transfer in fluidized beds consisting of coarse-grained particles (particle size generally $d_p > 2$ mm). The heat transfer is dominated by the heat transfer in the gap between the heated surface and the first row of particles adjacent to the heated surface. Consequently, the thermal properties of the particulate material will be irrelevant.

On the other hand, particle sizes $d_p \geqslant 2$ mm involve particle Reynolds numbers as high as $Re \geqslant 200$. In this case departure from the laminar flow regime can be expected. Therefore, an asymptotic solution, as derived for moving bed situations, i.e. of the type of stagnant fluid conditions ($Nu = \text{const}$), may no longer be applicable for fluidized beds consisting of coarse-grained particles. Instead, boundary layer effects become important.

REFERENCES

1. Molerus, O., Burschka, A. and Dietz, S., Particle migration at solid surfaces and heat transfer in bubbling fluidized beds—I. Particle migration measurement systems. *Chemical Engineering Science*, 1995, **30**, 817–877.
2. Dunsky, V. D., Zabrodsky, S. S. and Tamarin, A. I., On the mechanism of heat transfer between a surface and a bed of moving particles. *Proceedings of the 3rd International Heat Transfer Conference*, AIChE, 1966, Vol. 4, pp. 293–297.
3. Wunschman, J. and Schlünder, E. U., Wärmeübergang von beheizten Flächen an Kugelschüttungen. *Verfahrenstechnik*, 1975, **9**, 510–505.
4. Sullivan, W. N. and Sabersky, R. H., Heat transfer to flowing granular media. *International Journal of Heat and Mass Transfer*, 1975, **27**, 97–106.
5. Schlünder, E. U., Heat transfer to packed and stirred beds from the surface of immersed bodies. *Chemical Engineering and Processing*, 1984, **18**, 31–53.
6. Glosky, D., Glicksman, L. and Decker, N., Thermal resistance at a surface in contact with fluidized bed particles. *International Journal of Heat and Mass Transfer*, 1985, **27**, 599–610.
7. VDI-Wärmeatlas, Stoffwerte von Schüttungen, Chapter De, VDI, Düsseldorf, 5th edn, 1988.
8. Harakas, N. K. and Beatty, Jr, K. O., Moving bed heat transfer: I, effect of interstitial gas with fine particles. *Chemical Engineering Symposium Series*, 1963, **59**(41), 122–128.
9. Ernst, R., Wärmeübergang an Wärmetauschern im moving bed. *Chemie-Ingenieur-Technik*, 1960, **32**, 17–32.
10. Botterill, J. S., Butt, M. H. D., Cain, G. L. and Redish, K. A., The effect of gas and solids thermal properties on the rate of heat transfer to gas-fluidized beds. *Proceedings of the International Symposium on Fluidization*, Eindhoven, A. A. H. Drinckenburg (edit), 1967, pp. 442–457.
11. Barreto, G. F., Lancia, A. and Volpicelli, G., Heat transfer and fluid dynamic characteristics of gas-fluidized beds under pressure. *Powder Technology*, 1986, **46**, 155–166.